



Photophysical characterization of novel dipyrriene compounds based on pyrrolic hydrogen transfer

Zeliha Pınar Taşkıran, Gökhan Sevinç*

Department of Chemistry, Faculty of Science and Literature, Bilecik Şeyh Edebali University, 11230 Bilecik, Turkey

ARTICLE INFO

Article history:

Received 10 January 2022

Revised 7 March 2022

Accepted 7 March 2022

Available online 8 March 2022

Keywords:

Dipyrromethene

pH sensor

Visible region dyes

Linear absorption

Colorimetric sensor

ABSTRACT

In this work, we introduced novel dipyrromethene dyes which were synthesized in good yields from 2,4-diphenyl substituted pyrroles and aromatic aldehydes. The resulting structures were elucidated by NMR, FTIR and HRMS techniques. The absorption behaviors of the synthesized dipyrromethenes in various solvents and pH media were investigated by means of UV/Vis spectroscopy. It has been observed that the compounds with dipyrromethene skeleton respond very sensitively to pH changes in visible region. The compounds have two identical colors that vary according to the solvent and pH changings depending on pyrrolic proton. Their colors are dark green in the acidic region and vivid purple in the basic media. Presented study is important for the use of aryl substituted dipyrromethene compounds as dyes for colorimetric sensoric applications, as well as for the rational design of new dyes.

© 2022 Elsevier B.V. All rights reserved.

1. Introduction

Heterocyclic compounds known as dipyrromethenes or dipyrins are bidentate ligands in which two pyrrole rings are linked by a methylene bridge (Fig. 1) [1]. Although they were originally developed as precursors in the synthesis of porphyrins and other tetrapyrrole derivatives [2–4], they have become recognized in the synthesis of their fluorescent BF₂ complexes (commonly known as BODIPY) [5–9]. Besides, dipyrromethenes have been reported to form tetrahedral complexes with many metal ions particularly iron (II), iron (III), nickel (II), copper (II) and zinc (II) [10–13]. Although the completely non-substituted dipyrin is not stable at temperatures above –40 °C [14], its derivatives which have a phenyl group at –5 position (*meso*) are widely used in the literature [1].

Advances in the preparation of stable dipyrromethenes by the condensation of aromatic aldehydes with alkyl substituted pyrroles such as 2,4-dimethyl pyrrole or 2,4-dimethyl-3-ethyl pyrrole have greatly increased the versatility and usages of them. According to this method, dipyrins can be readily prepared by the oxidation of dipyrromethanes using 2,3-dichloro-5,6-dicyano-1,4-benzoquinone (DDQ) or p-chloranil as oxidative agents [15–17]. Although it is overshadowed by BODIPYs, which are the subject of many studies due to their chemical stability [18,19], fluorescence properties and intense light absorption capabilities in visible region [20–25], there are many unexplored areas remain about dipyrromethenes.

The fact that, susceptibility of the unsubstituted pyrrole ring positions ($-\alpha$ carbon atoms) to electrophilic and nucleophilic attacks causes dipyrins to be tend to polymerization, resulting in reaction yields losses [26,27]. It is therefore difficult to purify dipyrromethenes from the polymeric resinous by-products. In general, dipyrins are often difficult to purify by chromatography regardless of their preparation method. The use of alkyl substituted pyrroles partially prevents nucleophilic attacks, leading to an increase in synthesis yields, so commercial alkyl-pyrrole derivatives are preferred [26–28]. However, continuing the reaction using one-pot procedures led to the investigation of metal or boron complexes, not the dipyrromethenes themselves. Although it has been noted that the absorption spectra of some alkyl substituted dipyrromethene derivatives could change depending on solvent and protonation-deprotonation equilibria, there are very few studies in the literature [29,30]. Related studies cover the alkyl substituted analogues.

In this study, dipyrromethene derivatives **DPM-1** and **DPM-2**, containing substituted phenyl groups at –2 and –4 positions were synthesized using methods known in the literature [1,16,17,26]. In this context, firstly, pyrrole compounds as starting compounds with phenyl groups at –2, –4 positions of the heterocycle were synthesized in order to get elevated reaction yields, facilitate purification procedures and increase absorption intensities in the visible region. Afterward, by systematically changing donor methoxyphenyl groups to the *meso*, alpha ($-\alpha$) and beta ($-\beta$) positions of the dipyrromethene skeleton, the absorption behaviors of the compounds in different solvents and pH environments were investigated. pH-dependent photophysical properties of –1, –5, –9,

* Corresponding author.

E-mail address: gokhansevinc32@gmail.com (G. Sevinç).

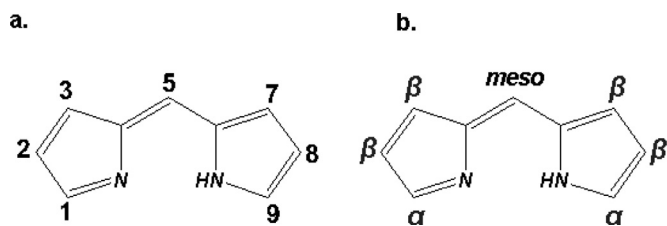


Fig. 1. Structure and IUPAC numbering of the dipyrromethene (a), alternative α/β nomenclature (b).

phenyl substituted dipyrromethene compounds have been studied. Herein, we wish to unveil a preliminary work on aryl-dipyrin systems, which are obtained in suitable yields and exhibit colorimetric properties depending on pH in both solid phase and solution.

2. Experimental

2.1. Materials and characterization

Benzaldehyde, acetophenone, 4-methoxy benzaldehyde, diethylamine and 4-methoxyacetophenone used in the synthesis of pyrrolic compounds were obtained from abcr chemicals co. while the other chemicals and solvents were obtained from Merck. Although all chemicals and solvents were used as received, dichloride methane was distilled over CaO prior to use. Qualitative follow-up of the reactions was made using thin layer chromatography and for this purpose TLC Silica gel plates (Merck, Kieselgel 60, 0.25 mm thickness) with F254 indicator were used and visualized by UV lamp. Purifications of the resulting dipyrins were accomplished by column chromatography using Merck Silica Gel 60 (230–400 mesh).

^1H NMR spectra were obtained in CDCl_3 solution at 400 MHz using a on a VARIAN Mercury spectrometer. Chemical shifts are expressed in ppm relative to residual CHCl_3 (δ : 7.24 ppm) in the deuterated solvent. ^{13}C NMR spectra were recorded in CDCl_3 , chemical shifts (δ) were given in ppm relative to solvent peaks (δ : 77.3) with TMS as internal reference. The coupling constants (J) were reported in Hertz. Melting points were measured by Stuart SMP30. Mass spectral analyses of the purified compounds were performed on an Agilent 6224 LC/MS-High Resolution Quadrupole Mass Time-of-Flight (HRMS) spectrometer without using a separation column. Isotope peaks of the proposed chemical structures were obtained by performing positive and negative ESI technique for pyrrole and dipyrromethene derivatives, respectively. The results are given in ppm in the synthesis sections. Perkin-Elmer 100 spectrometer (equipped with ATR unit) was used for FT-IR spectra of the compounds in the range 650–4000 cm^{-1} .

2.2. UV-Vis measurements in solution, pH studies and singlet oxygen characterization

The steady state UV-vis spectra of the dipyrromethene compounds were recorded on PG Instruments T-80 UV-Vis spectrophotometer. 1 cm quartz cells were used to perform general absorption measurements at 25 °C using undegassed samples. The solvents used in the preparation of the solutions were of analytical grade, except for water. Ultrapure water produced by reverse osmosis technique was used in the experiments. Baseline corrected UV-vis spectra were collected between 250 and 1100 nm. Measurements in different pH values were applied in $\text{CH}_3\text{CN}-\text{H}_2\text{O}$ (3:1, v/v) by adding 10^{-3} M of HCl to the dye solutions ($c = 3.0 \times 10^{-6}$ M) in a closed flask. The final pH values were measured using the calibrated Ohaus ST 300 pH-meter. During titration, the absorbance reading and pH values were taken after waiting 2 min for equi-

libration after each addition of titrant. The absorption spectra in different solvents were obtained by taking the stock solution at a certain concentration ($c = 3.4 \times 10^{-5}$ M) and then resolving it after removing the previous solvent. All solutions were kept in the dark during the measurement process. The pK_a acidity constants were obtained from the spectrophotometric titration curves [31] created by plotting the absorption intensities at certain wavelengths (612 nm and 662 nm for the **DPM-1** and **DPM-2**, respectively) vs pH of the solutions. The absorbance as a function of pH was obtained via non-linear curve fitting by Boltzman function, which provided the best fit to the data. Finally, pK_a was obtained from the pH value at the turning point. To examine the singlet oxygen generation properties of the compounds, experiments were performed in dichloride methane with 1,3-diphenylisobenzofuran (DPBF) as a chemical singlet oxygen trap [32,33]. The solutions were irradiated at 600 nm by a LED light source. The degradation of DPBF was monitored by absorption spectra at 414 nm and Φ_Δ values were calculated with the following equation:

$$\Phi_\Delta = \Phi_\Delta^{\text{ref}} \times \frac{k}{k(\text{ref})} \times \frac{F(\text{ref})}{F}$$

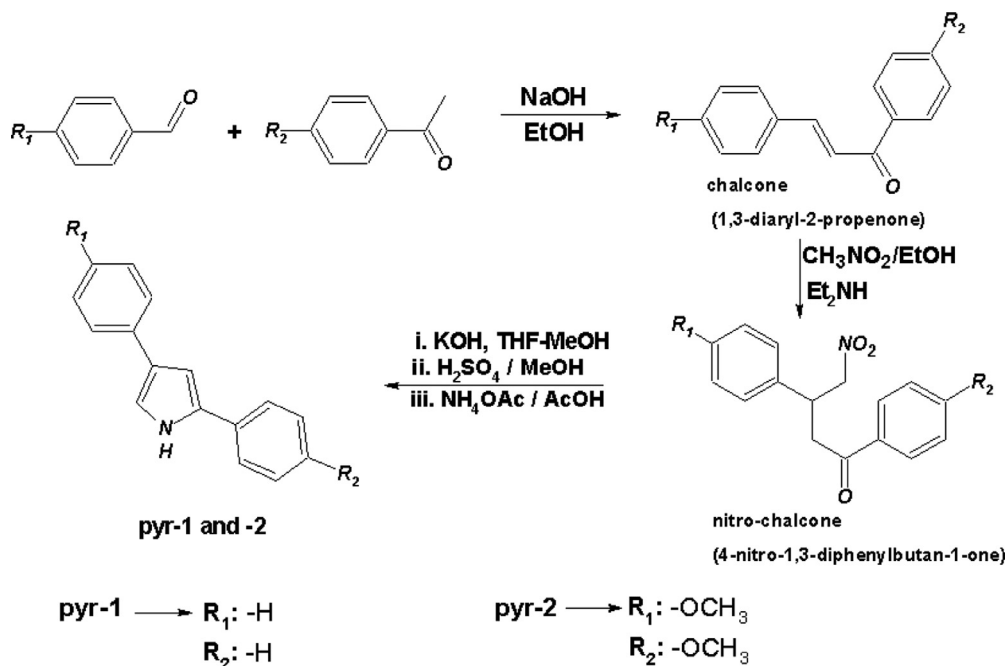
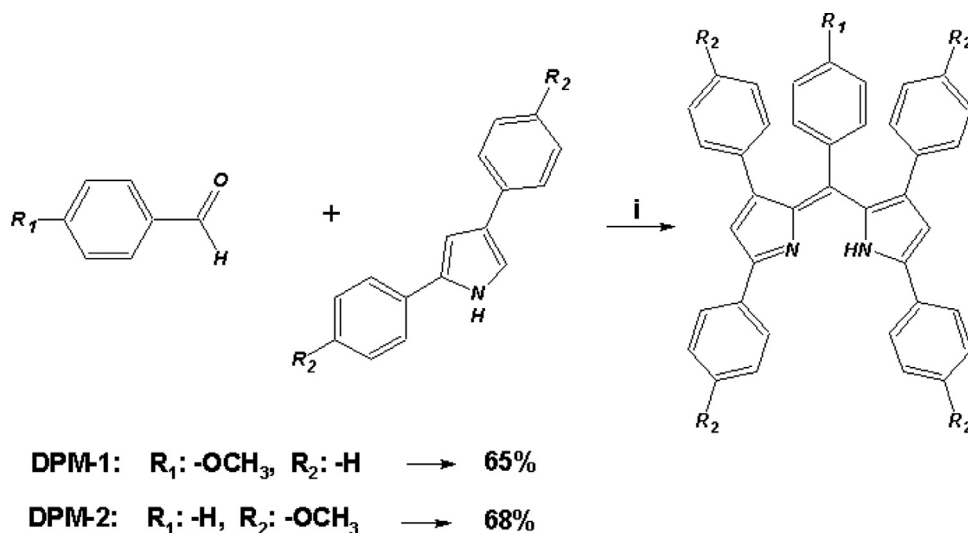
k and $k_{(\text{ref})}$ denote the rate constants of DPBF in the presence of reference methylene blue ($\Phi_\Delta = 0.57$ in DCM) and the sample, respectively. The slope of the lines were calculated by linear fit of the obtained data. F and $F_{(\text{ref})}$ are the absorption correction factors at excitation wavelength (600 nm), which is given by $F = 1 - 10^{-\text{Abs}}$. Abs refers herein to the absorbance of compounds and methylene blue (MB) at 600 nm.

2.3. Synthesis

The 2,4-diphenyl pyrrole derivatives were synthesized according to published procedures by using aromatic aldehyde and acetophenone derivatives as starting materials [34,35]. The synthetic pathway of the pyrrole derivatives **pyr-1** and **pyr-2** is shown in Scheme 1. The resulting compounds **DPM-1** and **DPM-2** were synthesized with respect to the literature [24,36,37] and related scheme was given in Scheme 2.

2.3.1. Synthesis of 2,4-diphenyl-1H pyrrole (pyr-1)

In a flat bottom flask with a stirring bar benzaldehyde (5.0 mL, 49.0 mmol) and acetophenone (6.30 mL, 54 mmol) were dissolved in 100 mL ethanol. Then, 5 mL of aqueous NaOH solution (20%) was added. The reaction mixture was stirred at room temperature for 24 h. The light-yellow precipitate formed was separated by filtration, washed with cold ethanol (10 mL) and left to dry in the open air. The resulting chalcone intermediate (9.70 g, 47.0 mmol) was dissolved in ethanol (100 mL) and nitromethane (12.8 mL, 0.24 mol) and diethylamine (24.8 mL, 0.24 mol) were added to the reflux for 12 h at 80 °C. At the end of this time, the reaction mixture was transferred to the rotary evaporator and evaporated until an oily substance remained. The nitro-chalcone intermediate was solidified in a vacuum oven. In a 500 mL flask, nitro-chalcone intermediate (8.59 g, 31.9 mmol) was dissolved in 300 mL of 1:1 methanol/THF (v/v) mixture and KOH (8.95 g, 0.16 mol) was added to it. It was stirred at room temperature for 2 h. The reaction mixture was then added dropwise with rapid stirring to 370 mL of 4:1 methanol/ H_2SO_4 (v/v) solution at -4 °C. At this stage, attention was paid to keep the temperature of the reaction mixture between 0–4 °C by using ice bath. When the addition was complete, the ice bath was removed and the mixture was stirred for another 2 h at room temperature. After this time, ice chips were added to the mixture, and then the mixture was neutralized to pH 6 with 5 M NaOH aqueous solution. The mixture was extracted with chloroform (50 mLx4) and the solvent was evaporated. The

Scheme 1. Synthetic route for the starting 2,4-diaryl pyrroles (**pyr-1** and **pyr-2**).Scheme 2. Synthetic route for the **DPM-1** and **DPM-2** (i: DCM, catalyst:TFA, rt, 12 h).

oily material was dried in a vacuum oven at 40 °C. The dried substance was taken into a flask and dissolved in 300 mL of AcOH, and NH_4OAc (24.6 g, 0.32 mol) was added and stirred at 100 °C for 2 h under reflux. The water was added to the mixture, which was cooled to room temperature, until the precipitation was complete (~300 mL). The heterogeneous mixture was filtered, the solid was air dried and the gray product **pyr-1** was purified by crystallization with chloroform:hexane solution. Yield: 3.43 g (32%), mp: 178–180 °C. FTIR (ATR, cm^{-1}) ν_{max} : 3194, 3024, 1665, 1549, 1480, 1271, 1013. ^1H NMR (400 MHz, CDCl_3): δ [ppm]: 8.43 (s, 1H), 7.59 (d, $J = 7.2$ Hz, 2H), 7.52 (d, $J = 8.0$ Hz, 2H), 7.42–7.36 (m, 4H), 7.27–7.20 (m, 2H), 7.13 (s, 1H), 6.85 (s, 1H). ^{13}C NMR (125 MHz DMSO-d_6) 136.2, 133.1, 133.0, 129.1, 129.0, 126.1, 125.5, 125.2, 125.0, 124.0, 117.1, 103.7. HRMS (Q-TOF-ESI) (m/z) Calcd: 219.1049 ($\text{C}_{16}\text{H}_{13}\text{N}$), found: 218.09832 [M-H] $^-$, $\Delta = 6.19$ ppm.

2.3.2. Synthesis of 2,4-bis[4-methoxyphenyl]-1H-pyrrole (**pyr-2**)

Prepared in the same manner as for **pyr-1**, using 4-methoxybenzaldehyde (5.0 mL, 41.1 mmol), 4-methoxyacetophenone (6.20 mL, 45.3 mmol), nitromethane (12.8 mL, 0.18 mol), diethylamine (18.6 mL, 0.18 mol), 250 mL 1:1 methanol/THF (v/v) mixture, KOH (7.05 g, 0.13 mol), 290 mL 4:1 methanol/ H_2SO_4 (v/v) solution, AcOH (250 mL), NH_4OAc (19.4 g, 0.25 mol); all reaction and purification conditions identical to above. Yield: 3.33 g (29%), mp: 218–219 °C. FTIR (ATR, cm^{-1}) ν_{max} : 3442, 1612, 1572, 1504, 1473, 1438, 1302, 1285, 1245, 1185, 1128, 1034, 835, 798. ^1H NMR (400 MHz, CDCl_3): δ [ppm]: 8.31 (s, 1H), 7.48 (d, $J = 8.8$ Hz, 2H), 7.44 (d, $J = 8.8$ Hz, 2H), 7.03 (s, 1H), 6.94–6.90 (m, 4H), 6.65 (s, 1H), 3.83 (s, 3H), 3.82 (s, 3H). ^{13}C NMR (125 MHz, DMSO-d_6) δ : 158.0, 157.5, 132.6, 129.1, 126.2, 126.0, 125.2, 124.9, 115.2, 114.6, 114.4, 102.3, 55.5, 55.4. HRMS

(Q-TOF-ESI) (m/z) Calcd: 279.12594 ($C_{18}H_{17}NO_2$), found: 278.11916 $[M-H]^-$, $\Delta=3.77$ ppm.

2.3.3. Synthesis of 2-[(3,5-diphenyl-2H-pyrrole-2-ylidene)(4-methoxyphenyl)methyl]-3,5-diphenyl-1H-pyrrole (DPM-1)

In a flat bottom flask with a stirring bar, 4-methoxy benzaldehyde (80 μ L, 0.65 mmol) and **pyr-1** (300 mg, 1.37 mmol) was dissolved in dry dichloromethane (70 mL) and N_2 was passed through for 5 min. To this solution, 1 drop of trifluoroacetic acid (TFA) was added, followed immediately by *p*-chloroanil (240 mg, 0.98 mmol). The reaction mixture was stirred at room temperature overnight. Depletion of the starting aldehyde was observed by TLC. The reaction mixture was concentrated about 25 mL on a rotary evaporator and filtered through a filter paper. The dark green filtrate was washed with water and extracted with $CHCl_3$ (3×30 mL). The solvent was evaporated, resulting solid was dried in open air and purification by column chromatography on silica gel eluting with chloroform-hexane (2:1, v/v) gave the product **DPM-1** as a dark green solid. Yield: 0.23 g (65%), mp: 113–114 °C. FTIR (ATR, cm^{-1}) ν_{max} : 3190, 1678, 1601, 1503, 1483, 1454, 1275, 1180, 1016, 920, 840, 765. 1H NMR (400 MHz, $CDCl_3$): δ [ppm]: 7.90 (s, 2H), 7.38–6.31 (m, 24H), 3.66 (s, 3H). HRMS (Q-TOF-ESI) (m/z) Calcd: 554.23582 ($C_{40}H_{30}N_2O$), found: 555.24209 $[M + H]^+$, $\Delta=2.81$ ppm.

2.3.4. Synthesis of 2-[-[3,5-bis(4-methoxyphenyl)-2H-pyrrol-2-ylidene](phenyl)methyl]-3,5-bis(4-methoxyphenyl)-1H-pyrrole (DPM-2)

Using a procedure identical to that described above benzaldehyde (52 μ L, 0.51 mmol) and **pyr-2** (300 mg, 1.01 mmol) were condensed in 50 mL dichloromethane to give **DPM-2**. 0.22 g (68%), mp: 93–94 °C. FTIR (ATR, cm^{-1}) ν_{max} : 3412, 2946, 1608, 1481, 1420, 1247, 1165, 1041, 927, 830, 717. 1H NMR (400 MHz, $CDCl_3$): δ [ppm]: 7.88 (d, $J = 7.6$ Hz, 2H), 7.78 (d, $J = 7.6$ Hz, 2H), 7.50–7.46 (m, 2H), 7.36–7.32 (m, 3H), 6.99 (s, 2H), 6.95–6.89 (m, 4H), 6.80–6.73 (m, 3H), 6.65–6.46 (m, 5H), 3.85–3.62 (m, 12H). ^{13}C NMR (100 MHz, $DMSO-d_6$): δ : 161.1, 153.6, 146.4, 143.3, 135.7, 132.3, 131.6, 130.7, 129.9, 129.6, 128.2, 127.9, 125.5, 114.4, 113.9, 113.5, 113.2, 55.4, 55.3, 55.2, 55.1. HRMS (Q-TOF-ESI) (m/z) Calcd: 644.26753 ($C_{43}H_{36}N_2O_4$), found: 645.27407 $[M + H]^+$, $\Delta=1.98$ ppm.

3. Results and discussion

3.1. Synthesis

The synthesis of the pyr-1 and pyr-2 consists of stepwise reactions and resulted in modest reaction yields (32% and 29%, respectively). The stages was passed by filtration and crystallization techniques without the need for column chromatography. The chalcone intermediate was obtained by aldol condensation, followed by the addition of nitromethane known as Michael addition [38,39]. In the last step, acidic hydrolysis of nitro chalcone derivatives by Nef reaction followed by their condensation reaction with ammonium source gave the 2,4-diphenyl pyrrole derivatives [38,39]. 1H NMR and HRMS support the two proposed structures such that integration and peaks are congruent. It was observed that both pyrrolic hydrogen atoms (on the α , β positions on the pyrrole ring) shifted to the upper field in 1H NMR due to the presence of electron-donating methoxy groups (6.85 and 6.65 ppm for the pyr-1 and pyr-2, respectively) as expected.

Dipyrromethene compounds **DPM-1** and **DPM-2** were obtained by the acid-catalyzed condensation reaction of the synthesized pyrroles and aromatic aldehydes at room temperature as given in Scheme 2. Since the aim is to examine the solvent and pH-dependent photophysical properties of the compounds if there are

Table 1

Photophysical parameters of **BDP-1** and **BDP-2** in THF.

Compound	λ_{max} abs/nm	ϵ_{max} Abs ($M^{-1}cm^{-1}$)	FWHM (nm)
DPM-1	535	23,530	87
DPM-2	553	24,940	100

electron donating phenyl groups in the alpha, beta and meso position of the dipyrromethene structure, **DPM-1** contains methoxy phenyl in the meso position while **DPM-2** contains phenyl group in the meso position and methoxy phenyl groups in other positions.

The synthesis method in question is well known in the porphyrin and bodipy chemistry [1,5,6,21]. However, in our preliminary experiments, in the first stage of the reaction, it was observed that the dipyrromethane intermediates were not formed by the known method, that is, the reaction did not progress. This problem was overcome by adding the oxidizing agent *p*-chloranil at the beginning of the reaction without waiting the formation of dipyrromethane intermediate with a simple modification by Duan et al. [36]. Shortly after the acid catalyst was added, the deep green color of the dipyrromethene derivative began to appear. As a result, **DPM-1** and **DPM-2** were obtained in good yields (65% and 68%, respectively), which are higher than when using alkyl substituted pyrroles such as 2,4-dimethyl pyrrole and Kryptopyrrole. Their relatively low efficiency can be attributed to increased by-product formation due to the chemical reactivity of the methyl protons at the alpha ($-\alpha$) positions of the pyrroles [26,27]. The crude products was purified by chromatography on silica column. Concentration of the reaction solution by slow evaporation of dichloromethane after termination of the reaction allowed precipitation of excess oxidizing reagent significantly facilitating subsequent column chromatography.

Although the synthesized compounds are soluble in high and medium polarity solvents such as chloroform, methanol, THF, their solubility in hexane is quite low. The identities of the compounds were confirmed by FTIR, HRMS, NMR spectroscopy. The 1H NMR spectra of the compounds showed characteristic peaks corresponding to the methoxy protons with additional aromatic phenyl proton signals of the substituted phenyl groups. Due to the intense aromatic groups in the structures, phenyl protons appeared as multiplets in the 6–8 ppm region, whereas the integration meets the expected structure. The selective signals in the compounds belong to the methoxy groups, which were observed as singlet peaks between $\delta = 3.62$ –3.82 ppm. In HRMS analysis, molecular ion peaks of both structures were observed as $[M + H]^+$, confirming the expected structures with a mass error of 2.81 and 1.98 ppm for the **DPM-1** and **DPM-2**, respectively. In the FTIR spectrum of compounds; aromatic C=C vibrations were observed intensely in the region between 1500–1700 cm^{-1} while C–N stretching vibrations were observed at 1275 and 1246 cm^{-1} , respectively. The aliphatic C–H stretching peaks are more prominent due to the number of methoxy groups below 3000 cm^{-1} for **DPM-2**.

3.2. Absorption properties of DPM-1 and DPM-2

The absorption characteristics of **DPM-1** and **–2** were determined based on the UV/Vis spectra taken in THF. The relevant spectrum is given in Fig. 2 and photophysical data are given in Table 1.

The spectrum of both dyes generally covers the range of 250–800 nm, but the main absorption bands are observed between about 440–640 nm. Absorption maximas belonging to S_0 – S_1 transitions are observed at 535 and 553 nm for **DPM-1** and **DPM-2**, respectively. In the UV/vis spectrum of **DPM-2**, 17 nm bathochromic shift is observed originating from the inductive effect of the donor methoxy groups. However, since the steric hindrance of the meso

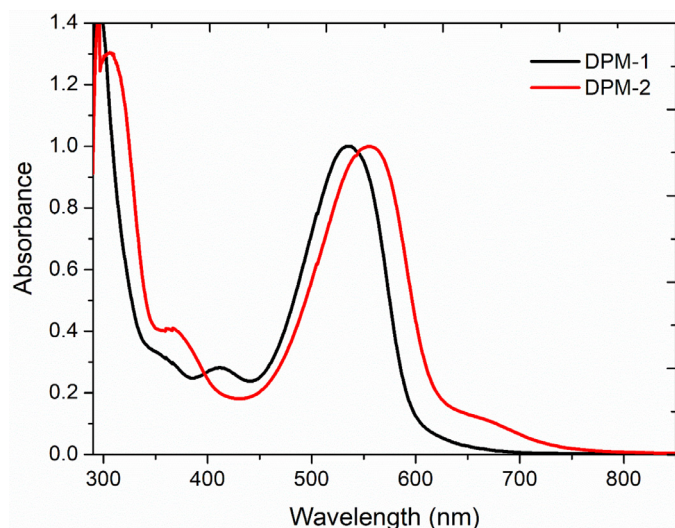


Fig. 2. Normalised UV/vis spectra of **DPM-1** and **DPM-2** in THF ($c: 3.4 \times 10^{-6} M$).

position restricts the conjugation of the methoxy phenyl groups attached to this position, the electron withdrawing/donor property of the substituent at this position does not cause a significant shift on absorption spectra [40,41]. Molar absorption coefficients are 23,530 and 24,940, respectively and show electron donating methoxy groups have limited effect on absorptivity. The wavelengths less than 410 nm belong to transitions of upper energy levels (S_2 , S_3 , ...). There are also strong bands belong to π - π^* transitions around 300 nm, consistent with the presence of intense phenyl groups. When compared to the boron difluoride complexes of dipyrromethenes; The shoulder peaks belonging to the vibrational transitions (0–1) of planar indacene core observed in the higher-energy part of the main absorption bands were not observed in these ligand-structured compounds [40]. In addition, significant increases in peak widths are obtained, such that the full width at half maximum values in BODIPY's, which generally vary in the range of 20–40 nm, increased to 87 and 100 nm at **DPM-1** and **-2**, respectively. This can be interpreted as absorption in a wider range of the visible region, but drastic declines in molar absorptivities should also be taken into account. While the molar absorption coefficients (ϵ) of BODIPYs are higher than 50 000 $M^{-1} cm^{-1}$ [5,42], those of these two compounds were calculated as 23,530 and 24,940, respectively. Although the absorp-



Fig. 4. Solutions of **DPM-1** in EtOH, EtOAc, THF and, DMF, respectively.

tion spectra of the related compounds in several organic solvents are similar, significant changes are observed in absorption profiles in EtOH. Normalized UV/Vis spectra taken in different solvents are given in Fig. 3a and 3b and their data are given in Table 2. The main absorption band of the **DPM-1** is localised between 532–535 nm depending on solvent. However, dramatic bathochromic shifts are observed in polar protic ethanol that absorption band shifts from 535 nm to 603 nm and the color of the solution changes markedly (Fig. 4). A similar situation applies to **DPM-2**. In comparison to **DPM-1**, bathochromic shifts of approximately 20 nm are observed in the absorption of **DPM-2** due to unrestricted methoxy phenyl groups at the $-\alpha$ and $-\beta$ positions of the dipyrin core.

As Guseva et al. noted [29], red shifting main absorption bands of the dipyrins in some solvents which have ability to form hydrogen bonding could be explained by specific solvation of the free base via hydrogen bonding with the heteroatoms. At the same time, the presence of the ionizable pyrrolic N–H proton in the dipyrin structures and the spectral shifts seen in the protic solvent could be indicated the importance of ambient pH. Therefore, the effect of pH was assessed by changing the solution pH from acidic to basic range by adding of aq. HCl and NaOH solutions in acetonitrile:water (3:1, v/v). The spectrophotometric pH titration spectra are shown in Fig. 5. Firstly, the response time observed due to pH change is quite short (less than 1 second). As seen in the Fig. 4, the

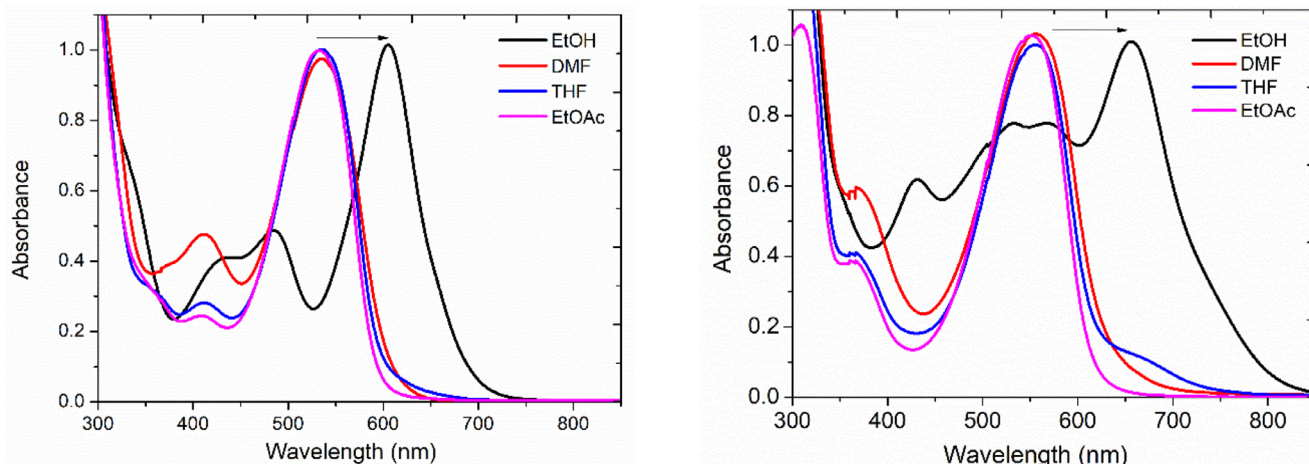


Fig. 3. Normalised UV/vis spectra of **DPM-1** (left) and **DPM-2** (right) in several solvents ($c: 3 \times 10^{-6} M$).

Table 2
Photophysical parameters of **DPM-1** and **DPM-2** in several solvents.

Compound →	Solvent	λ_{\max} abs/nm		ϵ max. Abs ($M^{-1}cm^{-1}$)		FWHM (nm)	
		DPM-1	DPM-2	DPM-1	DPM-2	DPM-1	DPM-2
	DMF	535	555	23,177	24,214	91	113
	EtOAc	532	550	23,201	23,900	87	100
	EtOH	603	655	23,870	25,120	76	297
	THF	535	553	23,530	24,940	87	100

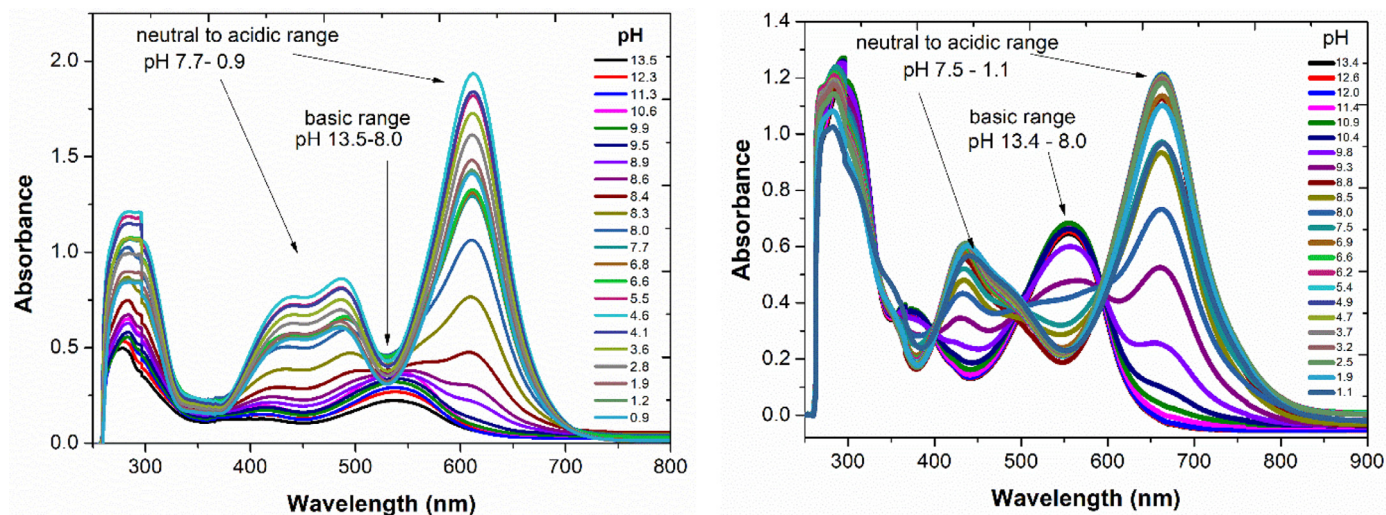


Fig. 5. pH dependent UV/Vis spectra of **DPM-1** (left) and **DPM-2** (right) in acetonitrile- H_2O (3:1, v/v).

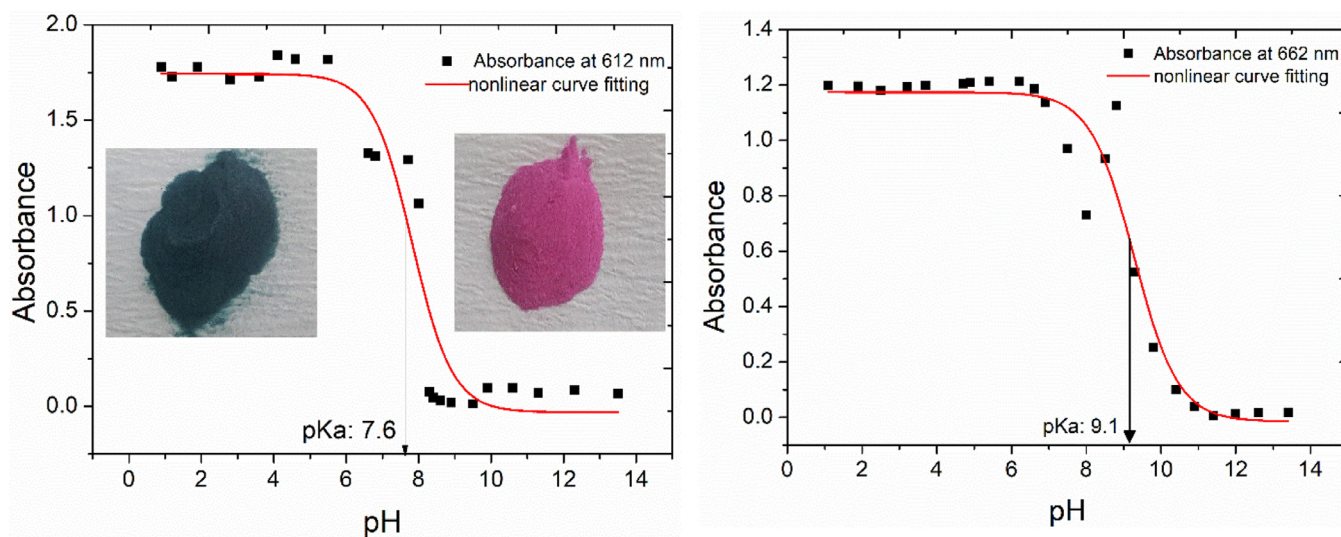


Fig. 6. Absorbance-pH profiles of **DPM-1** (left) and **DPM-2** (right) in acetonitrile- H_2O (3:1) (solid lines represent the best fit from the data pH vs absorbance at 612 nm and 662 nm for the **DPM-1** and **2**, respectively). The inside pictures are the acidic (green) and basic (pink) forms of the **DPM-1** adsorbed on silica gel).

absorption bands of **DPM-1** at 612 nm, 486 nm and 436 nm decreases with increasing pH and converges at about 538 nm to form a single broad band with lower absorption coefficient in acetonitrile- H_2O . Dramatical decreases are observed in the absorption intensities. The absorption band at 612 nm is taken as reference point, and when the absorption values at this wavelength are plotted against the ambient pH, it is seen that $pH = 7.6$ is the turning point in titration as in Fig. 6. Similarly, the absorption bands of **DPM-2** at 662 nm and 435 nm are completely quenched (Fig. 6b), resulting in new absorption band with a maximum of 560 nm emerge. In the titration of **DPM-2**, the pH at the turning point was calculated as 9.1. The pK_a of **DPM-2** increased from 7.6 to 9.1 compared to **DPM-**

1. Since the electron donating methoxy groups reduce the acidity of molecules, in this respect, it is compatible with the higher acid strength of **DPM-1**.

3.3. Singlet oxygen measurements

In recent years, studies on the application of new photosensitizer molecules in photodynamic therapy have been increasing. When present, singlet oxygen (1O_2) rapidly reacts with surrounding biomolecules, causing cellular damage that ultimately leads to cell death. Especially in halogenated compounds, high values are reached in singlet oxygen quantum yields (Φ_{Δ}) due to triplet for-

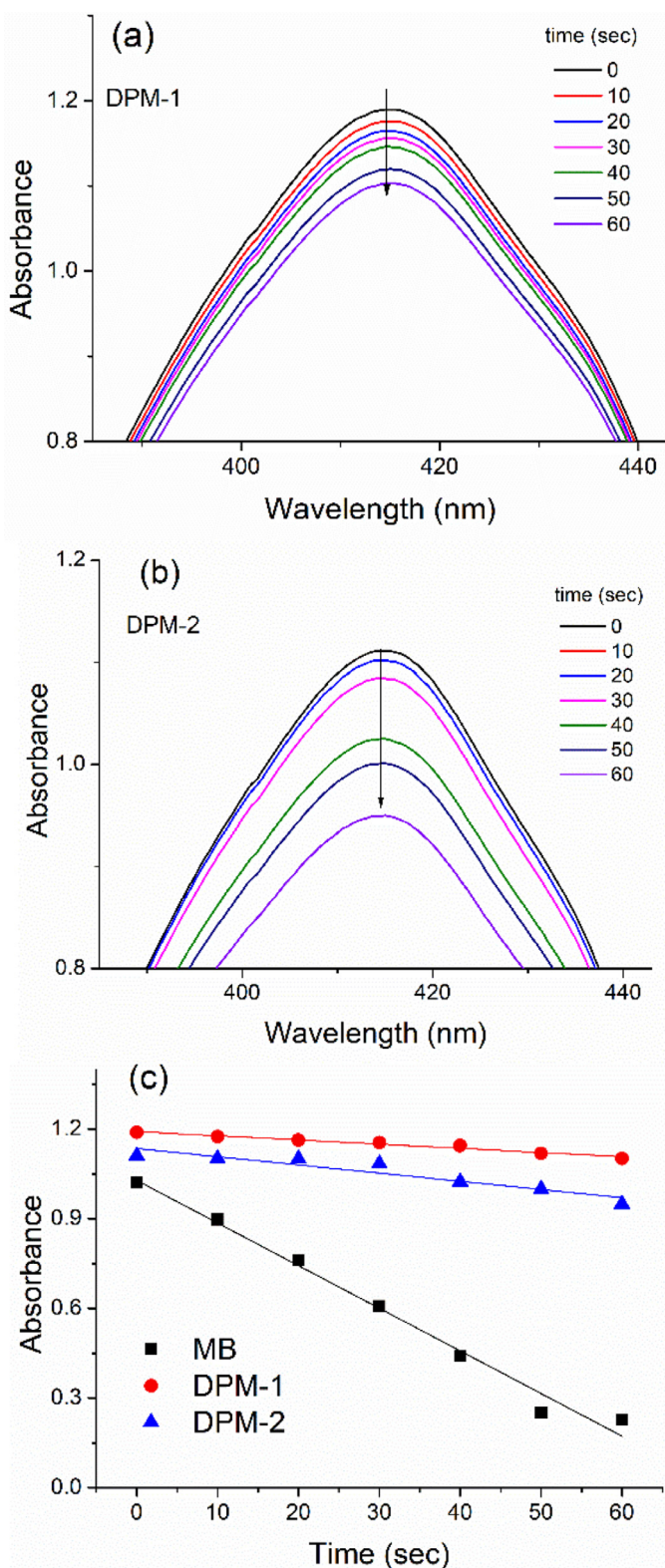


Fig. 7. Singlet oxygen characterization of **DPM-1** and **DPM-2**. (a) Absorption spectra of DPBF upon irradiation in the presence of the compounds **DPM-1** (b) **DPM-2** and (c) plot of change in absorbance of DPBF at 414 nm vs irradiation time ($\lambda_{\text{ex}} = 600 \text{ nm}$) against methylene blue (MB) as the standard in DCM.

mation as a result of heavy atom effect [23,24,43]. Herewith, singlet oxygen production efficiencies of the **DPM-1** and **-2** were also determined. For this purpose, the comparative method was used [32]. The changes of UV/Vis spectra of the chemical singlet oxygen trap molecule 1,3-diphenylisobenzofuran (DPBF) in the presence of **DPM-1** and **DPM-2** molecules in dichloride methane by irradiation at 600 nm and resulting DPBF decays at 414 nm against time are given in Fig. 7. The quantum efficiencies for singlet oxygen ($^1\text{O}_2$) of **DPM-1** and **-2** were calculated as 0.026 (2.6%) and 0.123 (12.3%) when methylene blue was used as a reference ($\Phi_{\Delta} = 0.57$ in DCM). Although the efficiencies of both compounds are low, the methoxy substituted **DPM-2** compound has increased value approximately 5 times compared to the **DPM-1**. The relevant compounds follow similar kinetics as seen in Fig. 6c. However, the higher absorption of **DPM-2** at the excitation wavelength (600 nm) resulted in a higher quantum yield of this compound. Although in its current form promising results have not been achieved, methoxy groups at position -1 , -3 , -5 and -7 of the core structure increases the absorptivity of the compound in visible region that resulted in higher singlet oxygen production.

4. Conclusions

Two novel aryl-substituted dipyrromethene compounds were synthesized. It was concluded that the use of phenyl substituted pyrrole derivatives causes an increase in the yield of dipyrromethene synthesis. Electron donating methoxyphenyl groups at $-\alpha$ and $-\beta$ positions of the dipyrin skeleton were found to cause bathochromic shift in the absorption wavelengths of the compounds. It was observed that the synthesized compounds were different in color in polar protic solvent, such that there was about 50 nm bathochromic shift in the absorption spectrum of the dyes in ethanol. Considering that the reason for this is the separation of the acidic pyrrole proton from the dipyrin structure, the absorption spectra of the compounds were taken at different pH values. As a result of the spectroscopic titration, it was determined that **DPM-1** had a turning point at pH: 7.6 and **DPM-2** at pH 9.1. Except these, by measuring the singlet oxygen quantum efficiencies of both compounds in dichloromethane, an increase accompanying the bathochromic shift was observed as a result of excitation at 600 nm. Although the singlet oxygen generation potential of the compounds are low, these values can be increased by changing the substituents and adding heavy atoms such as bromine to the 2,6 positions of the dipyrin core. Facile synthesis, higher synthesis efficiencies and easy purification procedures provide advantages for such aryl-substituted dipyrromethene compounds to be used as a target molecules as well as being ligands. In this study, it has been shown that dipyrromethene compounds can be used as pH sensors, and by making different synthesis designs, compounds suitable for different molecular recognition applications can be obtained.

Declaration of Competing Interest

The authors declare no conflict of interest.

Supplementary materials

Supplementary material associated with this article can be found, in the online version, at doi:[10.1016/j.molstruc.2022.132794](https://doi.org/10.1016/j.molstruc.2022.132794).

CRediT authorship contribution statement

Zeliha Pınar Taşkıran: Investigation, Writing – review & editing, Data curation. **Gökhan Sevinç:** Supervision, Conceptualization, Methodology, Investigation, Writing – review & editing.

References

- [1] R.S. Singh, R.P. Paitandi, R.K. Gupta, D.S. Pandey, Recent developments in metal dipyrroin complexes: design, synthesis, and applications, *Coord. Chem. Rev.* 414 (2020) 213269, doi:10.1016/j.ccr.2020.213269.
- [2] H. Fischer, Synthese des Hämins, *Naturwissenschaften* 17 (1929) 611–617, doi:10.1007/BF01506210.
- [3] R.B. Woodward, Total synthese des chlorophylls, *Angew. Chem.* 72 (1960) 651–662, doi:10.1002/ange.19600721803.
- [4] E. Sitte, M.O. Senge, The red color of life transformed—synthetic advances and emerging applications of protoporphyrin IX in chemical biology, *Eur. J. Org. Chem.* (2020) 3171–3191, doi:10.1002/ejoc.202000074.
- [5] A. Loudet, K. Burgess, BODIPY dyes and their derivatives: syntheses and spectroscopic properties, *Chem. Rev.* 107 (11) (2007) 4891–4932, doi:10.1021/cr078381n.
- [6] H. Lu, Z. Shen, Editorial: BODIPYs and their derivatives: the past, present and future, 2020. *Front. Chem.* 8, 290. doi:10.3389/fchem.2020.00290.
- [7] A.N. Kursunlu, M. Ozmen, E. Güler, A novel fluorescent chemosensor for Cu(II) ion: click synthesis of dual-bodipy including the triazole groups and bioimaging of yeast cells, *J. Fluoresc.* 29 (2019) 1321–1329, doi:10.1007/s10895-019-02456-3.
- [8] G. Ulrich, R. Ziessel, A. Harriman, The chemistry of fluorescent bodipy dyes: versatility unsurpassed, *Angew. Chem. Int. Ed.* 47 (2008) 1184–1201, doi:10.1002/anie.200702070.
- [9] A. Turksöy, D. Yildiz, E.U. Akkaya, Photosensitization and controlled photosensitization with BODIPY dyes, *Coord. Chem. Rev.* 379 (2019) 47–64, doi:10.1016/j.ccr.2017.09.029.
- [10] S.M. Cohen, S.R. Halper, Dipyrromethene complexes of iron, *Inorg. Chim. Acta* 341 (2002) 12–16, doi:10.1016/S0020-1693(02)01176-3.
- [11] S.R. Halper, M.R. Malachowski, H.M. Delaney, S.M. Cohen, Heteroleptic copper dipyrromethene complexes: synthesis, structure, and coordination polymers, *Inorg. Chem.* 43 (4) (2004) 1242–1249, doi:10.1021/jc0352295.
- [12] Y. Wang, Z. Xue, Y. Dong, W. Zhu, Synthesis and electrochemistry of meso-substituted dipyrromethene nickel(II) complexes, *Polyhedron* 102 (2015) 578–582579, doi:10.1016/j.poly.2015.10.020.
- [13] A. Thompson, D. Dolphin, Double-helical dinuclear bis(dipyrromethene) complexes formed by self-assembly, *J. Org. Chem.* 65 (23) (2000) 7870–7877, doi:10.1021/jo000886p.
- [14] K. Tram, H.A. Yan, S. Vassiliev, D. Bruce, The synthesis and crystal structure of unsubstituted 4,4-difluoro-4-bora-3a,4a-diaza-s-indacene (BODIPY), *Dyes Pigm.* 82 (3) (2009) 392–395, doi:10.1016/j.dyepig.2009.03.001.
- [15] R.W. Wagner, J.S. Lindsey, A molecular photonic wire, *J. Am. Chem. Soc.* 116 (21) (1994) 9759–9760, doi:10.1021/ja00100a055.
- [16] J.K. Laha, S. Dhanalekshmi, M. Taniguchi, A. Ambrose, J.S. Lindsey, A scalable synthesis of meso-substituted dipyrromethanes, *Org. Proc. Res. Dev.* 7 (2003) 799–812, doi:10.1021/op034083q.
- [17] C.H. Lee, J.S. Lindsey, One-flask synthesis of meso-substituted dipyrromethanes and their application in the synthesis of trans-substituted porphyrin building blocks, *Tetrahedron* 50 (39) (1994) 11427–11440, doi:10.1016/S0040-4020(01)89282-6.
- [18] G. Sevinç, M. Özgür, B. Küçüköz, A. Karatay, H. Aslan, H. Yılmaz, Synthesis and spectroscopic properties of a novel “turn off” fluorescent probe: thienylpyridine substituted BODIPY, *J. Lumin.* 211 (2019) 334–340335, doi:10.1016/j.jlumin.2019.03.058.
- [19] S. Mula, A.K. Ray, M. Banerjee, T. Chaudhuri, K. Dasgupta, S. Chattopadhyay, Design and development of a new pyrromethene dye with improved photostability and lasing efficiency: theoretical rationalization of photophysical and photochemical properties, *J. Org. Chem.* 73 (2008) 2146–2154, doi:10.1021/jo702346s.
- [20] N. Boens, V. Leen, W. Dehaen, Fluorescent indicators based on BODIPY, *Chem. Soc. Rev.* 41 (2012) 1130–1172, doi:10.1039/C1CS15132K.
- [21] G. Sevinç, B. Kucukoz, H. Yilmaz, G. Sirikci, H.G. Yaglioglu, M. Hayvali, A Elmali, Explanation of pH probe mechanism in borondipyrromethene-benzimidazole compound using ultrafast spectroscopy technique, *Sens. Actuators B-Chem.* 193 (2014) 737–744, doi:10.1016/j.snb.2013.12.043.
- [22] E. Teknikel, C. Unaleroğlu, Colorimetric and fluorometric pH sensor based on bis(methoxycarbonyl)ethenyl functionalized BODIPY, *Dyes Pigments* 120 (2015) 239–244, doi:10.1016/j.dyepig.2015.04.021.
- [23] H. Yilmaz, B. Kucukoz, G. Sevinç, S. Tekin, H.G. Yaglioglu, M. Hayvali, A Elmali, The effect of charge transfer on the ultrafast and two-photon absorption properties of newly synthesized boron-dipyrromethene compounds, *Dyes Pigments* 99 (3) (2013) 979–985, doi:10.1016/j.dyepig.2013.07.036.
- [24] B. Kucukoz, G. Sevinç, E. Yildiz, A. Karatay, F. Zhong, H. Yilmaz, Y. Tuel, M. Hayvali, J. Zhao, H.G. Yaglioglu, Enhancement of two photon absorption properties and intersystem crossing by charge transfer in pentaaryl boron-dipyrromethene (BODIPY) derivatives, *Phys. Chem. Chem. Phys.* 18 (19) (2016) 13546–13553, doi:10.1039/C6CP01266C.
- [25] G. Ulrich, R. Ziessel, Convenient and efficient synthesis of functionalized oligopyridine ligands bearing accessory pyrromethene-BF₂ fluorophores, *J. Org. Chem.* 69 (6) (2004) 2070–2083, doi:10.1021/jo035825g.
- [26] T.E. Wood, A. Thompson, Advances in the chemistry of dipyrroins and their complexes, *Chem. Rev.* 107 (5) (2007) 1831–1861, doi:10.1021/cr050052c.
- [27] A. Thompson, S.M. Crawford, Conversion of 4,4-Difluoro-4-bora-3a, a-diaza-s-indacenes (F-BODIPYs) to dipyrroins with a microwave-promoted deprotection strategy, *Org. Lett.* 12 (7) (2010) 1424–1427, doi:10.1021/ol902908j.
- [28] M. Kollmannsberger, T. Gareis, S. Heinel, J. Breu, J. Daub, Electrogenerated chemiluminescence and proton-dependent switching of fluorescence: functionalized difluoroboradiazas-indacenes, *Angew. Chem., Int. Ed. Engl.* 36 (1997) 1333, doi:10.1002/anie.199713331.
- [29] G.B. Guseva, E.V. Antina, M.B. Berezin, A.S. Semeikin, A.I. Vyugin, Electronic absorption spectra of alkyl-substituted dipyrromethenes and Biladienes-a, c in organic solvents, *Russ. J. Gen. Chem.* 72 (1) (2002) 126–130, doi:10.1023/A:1015318017581.
- [30] A. Amiri, I.M. Comeau, A. Thompson, Heteroleptic zinc dipyrromethene complexes, *J. Heterocycl. Chem.*, 43(2), 431–435. doi:10.1002/jhet.5570430225.
- [31] L.E.V. Salgado, C.V. Hernández, Spectrophotometric determination of the pKa, isobestic point and equation of absorbance vs. pH for a universal pH indicator, *Am. J. Anal. Chem.* 5 (2014) 1290–1301 10.4236/ajac.2014.517135.
- [32] H. Yilmaz, G. Sevinç, M. Hayvali, 3, 3,5 And 2,6 Expanded aza-bodipys via palladium-catalyzed suzuki-miyaura cross-coupling reactions: synthesis and photophysical properties, *J. Fluoresc.* 31 (2021) 151–164, doi:10.1007/s10895-020-02646-4.
- [33] R.H. Young, D. Brewer, R.A. Keller, Determination of rate constants of reaction and lifetimes of singlet oxygen in solution by a flash photolysis technique, *J. Am. Chem. Soc.* 95 (2) (1973) 375–379, doi:10.1021/ja00783a012.
- [34] M.J. Hall, S.O. McDonnell, J. Killoran, D.F. O’Shea, A modular synthesis of unsymmetrical tetraarylazadipyrromethenes, *J. Org. Chem.* 70 (14) (2005) 5571–5578, doi:10.1021/jo050696k.
- [35] R.E. Gawsley, H. Mao, M.M. Haque, J.B. Thorne, J.S. Pharr, Visible fluorescence chemosensor for saxitoxin, *J. Org. Chem.* 72 (2007) 2187–2191, doi:10.1021/jo062506r.
- [36] X. Duan, P. Li, P. Li, T. Xie, F. Yu, B. Tang, The synthesis of polarity-sensitive fluorescent dyes based on the BODIPY chromophore, *Dyes Pigments* 89 (2011) 217–222, doi:10.1016/j.dyepig.2010.03.007.
- [37] G. Sevinç, B. Küçüköz, A. Elmali, M. Hayvali, The synthesis of -1, -3, -5, -7, -8 aryl substituted borondipyrromethene chromophores: nonlinear optical and photophysical characterization, *J. Mol. Struct.* 1206 (2020) 127691, doi:10.1016/j.molstruc.2020.127691.
- [38] Y. Ge, D.F. O’Shea, Azadipyrromethenes: from traditional dye chemistry to leading edge applications, *Chem. Soc. Rev.* 45 (2016) 3846–3864, doi:10.1039/C6CS00200E.
- [39] A. Gorman, J. Killoran, C. O’Shea, T. Kenna, W.M. Gallagher, D.F. O’Shea, *In vitro* demonstration of the heavy-atom effect for photodynamic therapy, *J. Am. Chem. Soc.* 126 (34) (2004) 10619–10631, doi:10.1021/ja047649e.
- [40] W. Hu, X.F. Zhang, X. Lu, S. Lan, D. Tian, T. Li, L. Wang, S. Zhao, M. Feng, J. Zhang, Attaching electron donating groups on the meso-phenyl and meso-naphthyl make aryl substituted BODIPYs act as good photosensitizer for singlet oxygen formation, *J. Lumin.* 194 (2018) 185–192 Pages, doi:10.1016/j.jlumin.2017.10.018.
- [41] X.F. Zhang, N. Feng, Photoinduced Electron Transfer-based halogen-free photosensitizers: covalent meso-Aryl (Phenyl, Naphthyl, Anthryl, and Pyrenyl) as electron donors to effectively induce the formation of the excited triplet state and singlet oxygen for BODIPY compounds, *Chem. Asian J.* 12 (2017) 2447–2456, doi:10.1002/asia.201700794.
- [42] K. Zlatič, H.B.E. Ayouchia, H. Anane, B. Mihaljević, N. Bararić, T. Rohand, Spectroscopic and photophysical properties of mono- and dithiosubstituted BODIPY dyes, *J. Photochem. Photobiol. A: Chem.* 388 (2020) 112206 1 February, doi:10.1016/j.jphotochem.2019.112206.
- [43] A. Kamkaew, S.H. Lim, H.B. Lee, L.V. Kiew, L.Y. Chung, K. Burgess, Bodipy dyes in photodynamic therapy, *Chem. Soc. Rev.* 42 (1) (2013) 77–88, doi:10.1039/C2CS35216H.